Coastal Engineering 142 (2018) 1–8

Contents lists available at ScienceDirect

Coastal Engineering

journal homepage: www.elsevier.com/locate/coastaleng

Assessment of long-term impact of storm surges around the Korean Peninsula based on a large ensemble of climate projections

Jung-A. Yang[a,b,*], Sooyoul Kim[c], Nobuhito Mori[b], Hajime Mase[b]

[a] School of Civil, Environmental and Architectural Engineering, Korea University, 145 Anamro, Sungbuk-gu, Seoul, 02841, Republic of Korea
[b] Disaster Prevention Research Institute, Kyoto University, Gokasho, Uji, Kyoto, 611-0011, Japan
[c] Graduate School of Engineering, Tottori University, 4-101 Koyama-Minami, Tottori, 680-8552, Japan

ARTICLE INFO

Keywords:
Storm surge
Climate change
Large ensemble experiment
d4PDF
Korea Peninsula

ABSTRACT

This study assesses the long-term impact of storm surges due to typhoons around the Korean Peninsula (KP) resulting from climate change. Long-term projection is conducted based on the large ensemble experiments on so-called d4PDF for the past and +4 K future climate conditions over 5000 years by a single atmospheric global climate model developed by the Meteorological Research Institute of Japan. The use of a large ensemble is to enable one to obtain probabilistic future changes in low-frequency of extreme storm surge events. The properties of typhoons which may directly and indirectly have an effect on the KP in terms of past and future climate conditions is extracted from d4PDF. These are employed as the driving force in the projection of future storm surges around the KP. The storm surge heights (SSH) around the KP are projected to increase in the future climate except for around some areas in the south coast. The magnitude of future change of SSH varies spatially. The maximum variation was estimated to be 0.36 m (9.9%) with a 100-year return period in the west area of the southeastern coast of the KP. The locations of the areas vulnerable to storm surge shift to the north area of the western region and to the west area of the southern regions in the Korean Peninsula under the future climate. The characteristic of future change to areas where high SSHs will occur coincides with that of the typhoon tracks.

1. Introduction

Characteristics of severe tropical cyclones (hereafter, TCs) resulting from global climate change are expected to change future storm surge heights (hereafter, SSHs) depending on ocean basins and regions (Mori and Takemi, 2016). Projection of future TC activity and future SSHs based on results of ensemble climate experiments performed using a global climate model (hereafter, GCM) under future climate conditions is ready to start being used at the regional scale for disaster prevention against storm surge (Yasuda et al., 2014; Kim et al., 2017; Vousdoukas et al., 2016; Yang et al., Unpublished). However, there are some uncertainties in the projection of future TC activity and future SSHs, which become larger as the spatial scale of interest narrows.

These uncertainties are mainly caused by global warming scenarios, climate models, and internal variability. Effects of the first two factors on projections of TC activity and SSH have been previously estimated by other researchers and the fifth phase of the Coupled Modeling Intercomparison Project (CMIP5; (Taylor et al., 2012)) experiments. For the first factor, for example, Yang et al. (Unpublished) investigated how the multi-global warming scenarios and multi-patterns of sea surface temperature (hereafter, SST) influence typhoon properties and SSH on a regional scale focusing on the Korean Peninsula (hereafter, KP) using the outputs of six ensemble experiments by a single GCM. It is confirmed by all ensemble experiments that the number of strong typhoons is expected to increase and the locations of typhoon genesis and typhoon lysis are projected to shift to the northwest. The extent of each change is anticipated to vary with the global warming scenarios and the SST patterns. Extreme SSHs are more affected by the intensity and track of the typhoon than the frequency. For the second factor, there are uncertainties resulting from GCM performance associated with model resolution, model physics, model biases, SST pattern, atmosphere-ocean coupling, and so on. Recent studies have reported that future TC activity is projected differently depending on the model resolution used and have formed a wide consensus that GCMs with resolutions finer than 100 km may be adequate for assessing future TC activity (Murakami and Sugi, 2010; Murakami et al., 2012a; Strachan et al., 2013; Wehner et al., 2015). For that reason, the use of a multi GCM ensemble participating in CMIP5 is not a good way to assess the impact

* Corresponding author. School of Civil, Environmental and Architectural Engineering, Korea University, 145 Anamro, Sungbuk-gu, Seoul, 02841, Republic of Korea.
E-mail address: ja0903@korea.ac.kr (J.-A. Yang).

https://doi.org/10.1016/j.coastaleng.2018.09.008
Received 27 November 2017; Received in revised form 11 June 2018; Accepted 29 September 2018
Available online 01 October 2018
0378-3839/ © 2018 Elsevier B.V. All rights reserved.

of a storm surge because these models tend to project TC activity unrealistically due to their coarse resolution (Camargo, 2013). However, previous studies have had difficulty in evaluating extreme SSHs with long return periods beyond 100 years (long-term predictions which are required in coastal structure design) because of the lack of enough samples of storm surge events. The previous studies used dynamic modeling resulting in some limitations on experiments of shorter time slices. As the experiments typically cover a little more than 20–30 years, these conclusions only hold for SSHs with rather short return periods. On the other hands, among the three factors resulting in the uncertainties of projection for future SSH, there has been little research on the internal variability such as decadal variations in the ocean, interannual variability in the extratropical atmosphere, and intra-seasonal variation in the tropics, which is considered as one of the most important factors for a lower frequency of anomalous climate extremes (Deser et al., 2012; Kay et al., 2015).

In order to obtain a number of samples in localized rare events and to evaluate the uncertainty resulting from the internal variability, Mizuta et al. (2016) carried out an unprecedentedly large ensemble of climate simulations under past and future climate conditions using a high-resolution climate model of the Meteorological Research Institute with a 60 km horizontal resolution (hereafter, MRI-AGCM3.2H). Uncertainties caused by the model performance of MRI-AGCM3.2H have been previously validated (Murakami and Sugi, 2010; Murakami et al., 2012b, 2014; Ogata et al., 2016). From the output of such large ensemble simulations, probabilistic future changes in extreme events with low-frequency on local scales can be estimated directly without the application of statistical models such as generalized extreme value distributions. This large ensemble experimentation allow us to estimate long-year return SSHs with a low statistical uncertainty.

This study projects future SSH with a particular return period along the KP based on typhoon data extracted from the output of large ensemble experiments. The research methodology in this study is similar to that of Yang et al. (Unpublished) but taking a dissimilar climate forcing of future conditions. First, the reproducibility of the typhoon data is estimated by comparing it to the observed typhoon data, and future changes of the typhoon properties such as genesis numbers, tracks, and intensities are discussed. In addition, a series of storm surge simulations around the KP are conducted using the typhoon data. Storm surge levels with a particular return period, namely every 100-years and 500-years, are assessed on a regional scale and on specific points. The remainder of this study is organized as follows: Section 2 briefly introduces the large ensemble experiments used in this study and storm surge simulation conditions. Section 3 presents the results and discussions on the characteristics of typhoons affecting the KP under past and future climates as well as the projection of the future SSH on the KP coast. Conclusions are provided in Section 4.

2. Methodology

2.1. Outline of large ensemble climate experiments

One of the most important factors for long-term storm surge assessment is atmospheric forcing. Atmospheric reanalysis or hindcasts are generally used but we here pick up the long-term climate projection dataset to force an increase in the projection time scale in the factor of $O(10^2)$. Mizuta et al. (2016) carried out an unprecedentedly large ensemble experiment of climate simulations using an atmosphere general circulation model, MRI-AGCM3.2H. Two types of experiments were conducted: a past climate experiment and a future climate experiment. For each climate experiment, sea surface temperature (SST), sea-ice concentration (SIC), and sea-ice thickness (SIT) were employed as the lower boundary conditions. Concentrations of greenhouse gases (CO_2, CH_4, N_2O, and CFCs), ozone, and aerosols were set as the external forcing. The configurations for each climate experiment are summarized in Table 1. The past climate experiment from 1951 to 2010 was simulated with 100 ensemble members for which the lower boundary conditions and those initial conditions were perturbed. Small perturbations of the SST (δSSTs) based on the SST analysis error were added to the SIC in order to produce different initial conditions. The future climate experiment from 2051 to 2110 was conducted with 90 ensemble members, assuming the global-mean surface air temperature becomes 4 K warmer than the pre-industrial climate, as explained in the following paragraphs. The amplitude of the global warming corresponded to that at the end of the 21st century based on the Representative Concentration Pathway 8.5 (RCP 8.5) scenario of CMIP5 and was held constant throughout the experimental period. By doing this, large samples can be obtained under the same specified circumstance of global warming. As for the boundary conditions, climatological SST warming patterns (△SSTs) were added to the observational SST after removing the long-term trend component. To set different initial conditions for each ensemble member, 15-member ensemble experiments using different δSSTs of the past simulation were conducted with six △SSTs.

Outputs of each simulation are available to the public in a database called the “Database for Policy Decision-Making for Future Climate Change (code name: d4PDF)”. The d4PDF aims to be utilized for the impact assessment of hazards and adaptation planning for global warming. This study used the outputs in d4PDF. Hereafter, each output under the past and future climate conditions will be abbreviated as $d4PDF_{past}$ and $d4PDF_{future}$, respectively. Typhoon data extracted from the outputs, which were identified through tropical cyclone detection (Murakami et al., 2012a), was employed as external forcing for a storm surge simulation in the KP. This study was concerned with typhoons affecting the KP that pass through the area of 32–40°N and 122 to 132°E (shown by a solid rectangle with purple color in Fig. 1 (left)).

2.2. Storm surge simulation conditions

A variety of storm surge projections for the typhoon events from the d4PDF was carried out using a coupled model of surge, wave, and tide (SuWAT; (Kim et al., 2008)). In this study, only the surge module was used so as to reduce the computational cost. Flooding was not considered. All simulations were conducted with spin-up runs for 48 h prior to the calculation of the typhoon event so as to obtain stability of the sea surface level and the current over the entire computational domain. Pressure and wind fields for a typhoon event were produced using the parametric wind and pressure models of Fujita (1952) and Fujii and Mitsuda (1986), which are embedded in the SuWAT, respectively. The parameters of the date, the typhoon position (longitude and latitude), the minimum central pressure (hPa) and the moving speed (km/h) were estimated from d4PDF to generate the atmospheric fields. The radius from the center of typhoon to the point of maximum wind (R_{max}), which is not provided by d4PDF, was calculated using an empirical formula proposed by Yasuda et al. (2010) based on the parameterization method. Since the purpose of this study was to analyze the effects of climate change on future changes of typhoon and storm surge characteristics, it is assumed that the statistical characteristics between R_{max} and atmospheric central pressure are identical for both present and future climate conditions. The empirical formula was also applied in order to estimate the R_{max} of future typhoons.

Four-domain nesting with a 1:3 ratio of spatial grid size from coarse grids to fine grids was applied (refer to the dashed rectangles in Fig. 1). The outermost domain (D1) is set in the region of 20°–42°N, 117° to 132°E, where it nearly covers the formation and dissipation of typhoons approaching the KP. The innermost domain (D4) is the region 33.5° to 35.75°N, 127° to 130°E which has historically been one of the more surge-prone areas in the KP (Yang et al., 2017) and is defined here as the southeastern area of the KP. D4 has a spatial resolution of 0.008333° (approximately 760 m). Details on each calculation domain are shown in Table 2. Bathymetry data in D1 were downscaled from the General Bathymetric Chart of the Oceans (GEBCO, 2003). For the

Table 1
Configuration for each climate experiment.

		Historical simulation	Future simulation (+4 K warming)
Climate experimental period		From 1951 to 2010 (60 years)	From 2051 to 2110 (60 years)
Ensemble members		100	90
Low boundary condition	SST	observed	observed SST + climatological SST warming patterns (△SSTs)
	SIC	COBE-SST2	adjusted one to match future SST
	SIT	climatological monthly SIT	adjusted one to match future SST
External forcing	Greenhouse gases	observed	values at 2090 under RCP 8.5
	Ozone	monthly output form MRI-CCM	2090 output form MRI-CCM
	Aerosols	monthly output from MRI-CGCM	2090 output from MRI-CGCM

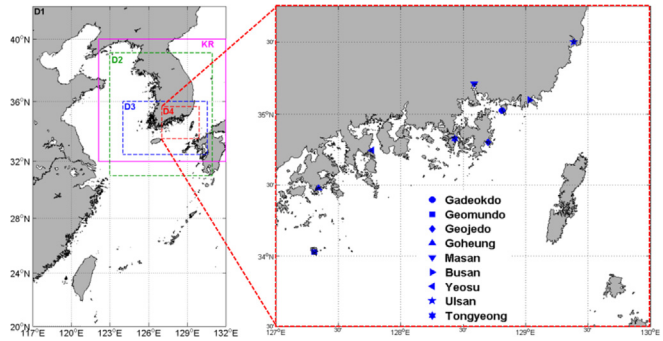

Fig. 1. Definition area for typhoons affecting the Korean Peninsula (abbreviated as "KR" written in purple on the upper right corner) on the left panel and calculation domains for storm surge projections (abbreviated as "D#", # is the number of domain) and (right) tidal observation stations in D4 on the right panel.

Table 2
Information on each calculation domain.

# of Domain	The range of domain	The grid size	# of grids
1	117°E ~ 132°, 20°N ~ 42°N	Δx = 9059.8 m, Δy = 11,560.5 m	151 × 211
2	123°E ~ 131°, 31°N ~ 39°N	Δx = 4563.2 m, Δy = 5547.1 m	160 × 160
3	124°E ~ 130.5°, 32.5°N ~ 36°N	Δx = 2281.8 m, Δy = 2773.2 m	260 × 140
4	127°E ~ 130°, 33.5°N ~ 35.75°N	Δx = 760.7 m, Δy = 924.5 m	360 × 270

remaining nested domains, the Digital 30 s Gridded Bathymetric Data of the Korea Marginal Seas dataset (Seo, 2008), which is one of higher resolution bathymetric datasets, was used. The time step used for storm surge computation was five minutes.

3. Results and discussion

3.1. Typhoon characteristics under the past and the future climate conditions

Typhoon characteristics such as the genesis number, track, and minimum central pressure in past climate conditions around Korea were examined by comparing the typhoon data from the $d4PDF_{past}$ with those of the observed typhoon dataset (IBTrACS; (Knapp et al., 2010)), while the global change in typhoon characteristics by d4PDF was analyzed by Yoshdia et al. (Yoshida et al., 2017). Moreover, future change was assessed by comparing typhoon data of the $d4PDF_{past}$ to that of the $d4PDF_{future}$.

3.1.1. The number of the typhoons

First, the reproducibility of the typhoons affecting the KP were evaluated in the past climate and in its projected future change. The

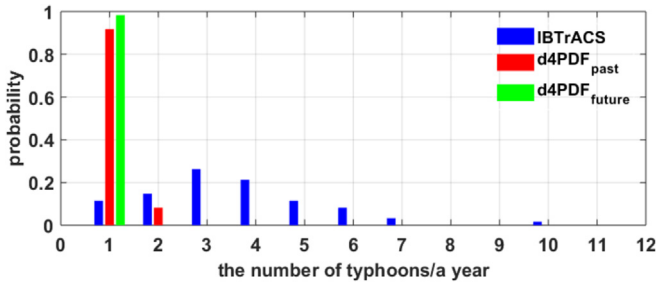

Fig. 2. Probabilities of annual number of typhoons passing around the Korean Peninsula. (a) Observations (IBTrACS) from 1961 to 2010, (b) ensemble member mean of simulations under past climate condition ($d4PDF_{past}$) from 1961 to 2010 and (c) ensemble member mean of projections under future climate condition ($d4PDF_{future}$) from 2061 to 2110.

probabilities of the occurrence of particular annual numbers of typhoons around the KP in the past and future climate conditions are presented in Fig. 2. The total number of typhoons around the KP under the past climate conditions are 214 (3.56/year) and 6475 (1.08/year/member) for IBTrACS and $d4PDF_{past}$, respectively. The $d4PDF_{past}$ results underestimate the number of typhoons around the KP. Note that the tropical cyclone detection method by Murakami et al. (2012a) used in this study is calibrated so as to match the observed annual cyclogenesis global number. Yasuda et al. (2014) examined the annual number of typhoons from MRI-AGCM3.2 with a 20 km resolution in the Northwest Pacific basin using the same tropical cyclone detection method and reported it to be ± 0.5 per year less than the observed number (Knapp et al., 2010). Although the annual number of typhoons affecting the KP is underestimated, the large ensemble experiments produced large samples of storm surge events. That makes it possible to evaluate rare SSH events with a return period of more than several decades for the design of coastal disaster prevention structures.

The total number of typhoons affecting the KP in the future climate condition is projected to be 3632 (0.67/year/member), while in the past climate condition it is 6475 (1.08/year/member). It was found that the number of typhoons approaching the KP is significantly reduced in the future climate condition by 38%. This value is the same as the results with Cluster 2 and Cluster 3 of the CMIP5 SST patterns under the RCP8.5 scenario using the same MRI-AGCM3.2H from Yang et al. (Unpublished).

3.1.2. Tracks of the typhoons

Next, the features of the typhoon tracks under the past and future climate conditions were assessed. Fig. 3 expresses the typhoon tracks as annual mean ratios of the number of typhoons in each calculation grid. The reproducibility of the typhoon tracks from $d4PDF_{past}$ was analyzed based on Fig. 3 (a) and (b). Typhoons which were generated in both the areas of 5°–20°N and 113° to 170°E go west in the South China Sea and change their path to the northeast toward the KP near Taiwan. Afterward, they approach the western and southern coasts of the KP. The tracks from $d4PDF_{past}$ reproduce those from IBTrACS well. The continuous distribution of typhoon movement by grid was obtained by

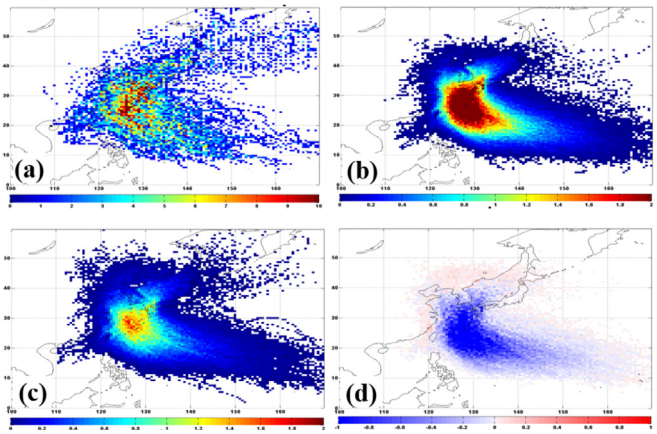

Fig. 3. Annual number of typhoons affecting the Korean Peninsula passing through each calculation grid: (a) observations (IBTrACS), (b) ensemble member mean of simulation under past climate conditions ($d4PDF_{past}$), (c) ensemble member mean of projection under future climate conditions ($d4PDF_{future}$) and (d) change between $d4PDF_{past}$ and $d4PDF_{future}$. Blue and red colors in legend of (d) refer to decreases and increases, respectively.

virtue of the abundance of typhoon data available in $d4PDF_{past}$.

A future change of typhoon track was evaluated based on Fig. 3 (b) and (c). The general typhoon tracks including the locations of typhoon genesis and lysis are projected to shift to the northwest in the future. The typhoons currently change their trajectories to the northeast near Shanghai, which is north of Taiwan. Fig. 3 (d) shows the differences in the number of typhoons passing through each calculation grid. Under future climate conditions the number of typhoons affecting the KP is expected to decrease while the number of typhoons passing through the regions above 40°N and to the left of 120°E, is anticipated to increase. These projected characteristics of future tropical cyclone track shift are similar to those of Mori and Takemi (2016), although the given scenario is different.

3.1.3. Minimum central pressures of the typhoons

Finally, the minimum central pressure was analyzed. The probability and probability density function of the minimum central pressure are indicated in Fig. 4. Mean values of the minimum central pressure are 981.7 hPa and 971.4 hPa for IBTrACS and $d4PDF_{past}$, respectively (see Fig. 4 (d)). The difference between both is about 10.4 hPa. The mean value of minimum central pressure from $d4PDF_{past}$

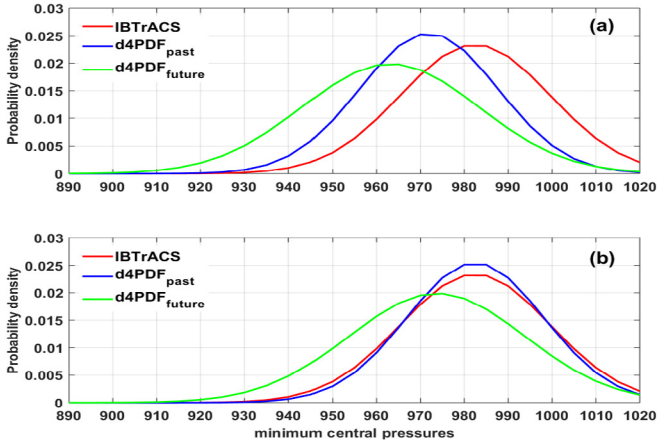

Fig. 4. Probability density functions of minimum central pressures of typhoons affecting the Korean Peninsula: (a) without the correction of bias between observations (IBTrACS) and large ensemble simulation under past climate conditions ($d4PDF_{past}$) and (b) with bias correction. Red, blue, and green lines in each panel indicate IBTrACS, $d4PDF_{past}$ and $d4PDF_{future}$, respectively.

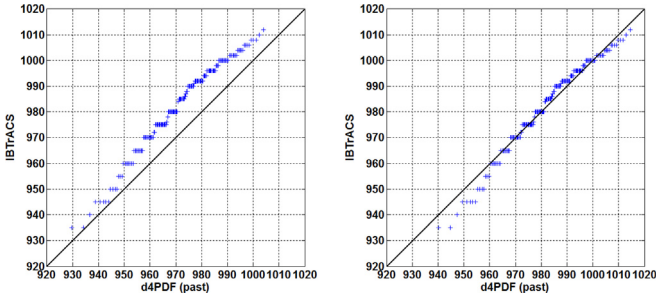

Fig. 5. Quantile-quantile (q–q) plots of minimum central pressures between observations (IBTrACS) and large ensemble simulations ($d4PDF_{past}$): without the correction of bias between IBTrACS and $d4PDF_{past}$ (left) and with bias correction (right).

is smaller than 10.4 hPa. It was reported that MRI-AGCM3.2H is inclined to have a lower central air pressure due to its weak representation of wall cloud (Mori and Takemi, 2016). In fact, the results of ensemble experiments using the same GCM model used in previous studies (Yasuda et al., 2014; Yang et al., Unpublished) have shown similar results. However, this difference cannot be neglected when projecting storm surges (Harris, 1963). A statistical bias correction was applied to the minimum central pressure value from $d4PDF_{past}$ to adequately assess the typhoon intensity, since the parametric wind and pressure models were used for generating atmosphere fields. To examine whether two data sets of the minimum central pressures of the typhoons between IBTrACS and $d4PDF_{past}$ come from populations with a common distribution, the quantile-quantile (q-q) plot of those with a 45-degree reference line is shown in Fig. 5. Before the calibration of values of the minimum central pressure from $d4PDF_{past}$, points representing the relationship of the minimum central pressure between the two data sets are in a straight line above the 45-degree reference line. That indicates that the two data sets come from populations whose distributions differ only by a shift in location. So, the minimum central values from $d4PDF_{past}$ and $d4PDF_{future}$ were linearly calibrated. Following this calibration, the points are approximately on the reference line. In other words, the probability distribution for $d4PDF_{past}$ is consistent with that for IBTrACS.

Mean values of the minimum central pressures for $d4PDF_{past}$ and $d4PDF_{future}$ after bias correction are 981.7 hPa and 973.5 hPa (refer to Fig. 4 (d)), respectively. The projected future change in the mean values is about 8.2 hPa. Typhoons under the future climate conditions are stronger than the ones that occurred under the past climate conditions. Furthermore, the significant projected future change of the minimum central pressure is evident when intensifying typhoons whose pressures are smaller than 940 hPa.

From the discussion above, under the past climate conditions, the number of typhoons affecting the KP was underestimated compared to the observations, while the general trend of the tracks of them was consistent with that of the observations. The mean value of the minimum central pressure of them was also smaller than that of the observations by 10.4 hPa. Since this difference cannot be neglected in projecting future SSHs (Harris, 1963), the mean values for d4PDF were linearly calibrated. The bias-corrected values will be used to project future storm surges. Under the future climate conditions, the number and intensities of the typhoons affecting the KP are anticipated to decrease and increase, respectively. In addition, the general typhoon track is projected to shift to the northwest. Note that this projection of the future characteristics of the typhoons affecting the KP was derived from a single GCM output. Sterl et al. (2009) reported that different GCMs employing different parameterizations could produce different atmospheric fields. Yasuda et al. (2014) examined the accuracy of typhoon data from two versions of MRI-AGCM which are named 3.1S and 3.2S compared to observed data. MRI-AGCM3.2S, which is the same model as ours with a different resolution, is the upgraded version of MRI-

AGCM3.1S employing new schemes and parameterizations. The typhoon data from MRI-AGCM3.2S shows better reproducibility in terms of typhoon characteristics than MRI-ACCM3.1S. It is also indicated that the cumulus convection scheme is the most effective factor improving the reproducibility of cyclogenesis in the Northwest Pacific. Section 3.2 describes the future SSHs with specific return periods on the KP coast and at particular points in the KP.

3.2. Projection of future storm surge heights around the Korean Peninsula

A series of storm surge simulations was conducted using selected strong typhoons in d4PDF with minimum central pressures of 970 hPa or less so as to reduce computational costs. The magnitude of storm surge is influenced by typhoon conditions such as atmospheric pressure differences, horizontal gradient of atmospheric pressure, maximum sustained winds, approach direction, landfall location and duration time. This study focused only on the projection of storm surge heights caused by higher intensity typhoons as defined by the minimum central pressure. The number of selected typhoons was 1428 in the past climate and 1522 in the future climate, which correspond to 6000 years and 5400 years of data, respectively. Maximum SSHs on each calculation grid for every typhoon event from the simulation results were used as the maximum value data for the extreme value statistical analysis in order to evaluate the future storm surge risk to the KP over long periods.

A standard frequency estimation procedure is as follows (Hamdi et al., 2014): (1) verifying randomness, homogeneity, and stationarity hypotheses of data as well as detecting outliers, (2) calculating empirical probabilities of exceedance using sorted and ranked data, (3) fitting a curve to these data with distribution functions and selecting the best distribution to represent these data and (4) estimating the extreme value with the return period R of interest applying extrapolation or interpolation based on (3). The return period of R-year of an event is calculated as following:

$$R = \frac{1}{\lambda(1-P)} \tag{1}$$

where λ is the annual average incidence of events and P is the cumulative probability. Generally, when estimating the probability values of SSH with a particular return period, extreme value distributions such as Gumbel, Fréchet, or Weibull distributions are employed in step (3) in order to calculate P because of the low maximum value of data for evaluation. However, in this study, the probability value P was directly calculated (i.e. through nonparametric statistical analysis) by applying a plotting position formula without extrapolation based on any distributions function. Of several available plotting position formulas, in this study, the Weibull formula (Weibull, 1939) in Eq. (2) was employed following the recommendations of Makkonen (2006).

$$P = \frac{m}{N+1} \tag{2}$$

where P is the cumulative probability associated with the m-th smallest value of the maximum SSHs data, m is the rank of the value of the maximum SSHs, which has a value of 1 for the largest value, and N is the total number of the maximum SSHs. SSHs with specific return periods under the past and future climate conditions are assessed qualitatively on regional scales (D2, D4 in Fig. 1 (left)) and quantitatively on specific points in D4 (refer to Fig. 1 (right)).

First, the extreme SSHs around the KP are estimated by the above-mentioned nonparametric method. Fig. 6 shows spatial distributions of the SSHs with the 100-year return period under the past and future climate conditions as well as the future change of SSH. Under the past climate, higher SSHs are distributed in the center areas of the western region and the southern region in the KP. On the other hand, the locations of the areas vulnerable to storm surge under the future climate shift to the northern area of the western region (where the capital area, including Seoul, is located), and to the western area of the southern regions in the KP. This characteristic of future change to areas where there will be higher SSHs mainly occurs due to the combination of typhoon track shifts and their intensity changes. The SSH around the KP is projected to increase under the future climate conditions except for in some areas on the south coast. The magnitude of the future change of SSH varies spatially due to changes in the typhoon characteristics changes and local amplification.

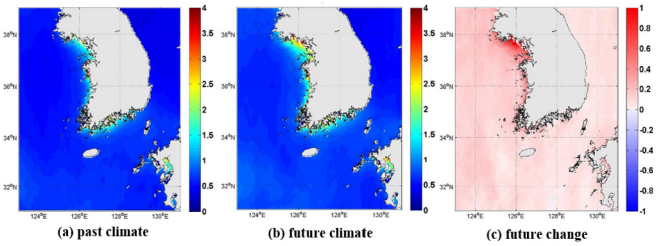

Fig. 6. Spatial distributions of storm surge heights (m) around the Korean Peninsula (D2) with a 100-year return period. (a) The past climate, (b) the future climate, and (c) future changes.

Yasuda et al. (2014) conducted the scenario-based projection, SRES A1B, of future SSHs in East Asia including the KP based on the output using MRI-AGCM3.2S. They reported that SSHs around the KP under future climate conditions would increase along the south coast and decrease along the west coast, which is in disagreement with our findings. They conducted similar scenario-based projections using the same AGCM but the periods of projections are 25-year time-slices for the past and future climates. Therefore, there are small numbers of typhoon events at particular locations, although they examined the extreme value analysis for 100 year return events from the output for 25-year time-slice experiments. Only a few typhoons have reached the KP according to the 25-year time-slice experiments. Note that there is a difficulty in direct quantitative comparison between their experiments and ours because of the different areas of interest studied: They discussed the reproducibility of typhoons in the Northwest Pacific region and the future changes of SSHs in East Asia. Therefore, this study performed a qualitative analysis. Although the mean value of the minimum central pressure of typhoons extracted from the output was underestimated compared to that of the observation typhoon dataset, they used typhoons without correction for the minimum central pressure. For the reasons mentioned, disagreement between our findings and theirs resulted from the number of ensemble experiments, the reproducibility of typhoons. and the calibration of the minimum center pressure of typhoons.

Next, the results for the southeastern area of the KP with complex topography are discussed based on a higher resolution nesting domain. Fig. 7 presents spatial distributions of SSH with the 100-year return period under the past and future climates as well as the projected future change of SSH. From Fig. 7 (a), it can be seen that the higher SSHs take place in the west and center area, and that most severe SSH occurs in a bay (marked with “A” in Fig. 7 (a)) with 3.62 m. Most areas of the west will be projected as vulnerable to storm surge under the future climate conditions as described in Fig. 7 (b). The value of the highest SSH is

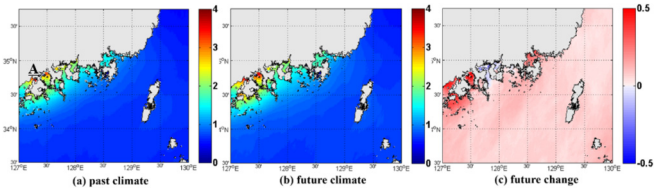

Fig. 7. Spatial distributions of storm surge heights (m) in the southeastern area of the Korean Peninsula (D4) with a 100-year return period. (a) The past climate, (b) the future climate, and (c) future changes.

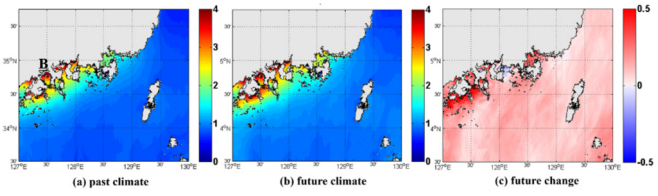

Fig. 8. Spatial distributions of storm surge heights (m) in the southeastern area of the Korean Peninsula (D4) with a 500-year return period. (a) The past climate, (b) the future climate, and (c) future changes.

estimated at 3.98 m in the bay. As shown in Fig. 7 (c), the SSH for overall areas increases under the future climate compared with those under the past climate, except for in some areas ranging between 127.5 °E to 128 °E and 34.6 °N to 35 °N. A pronounced increase of the SSH is projected to take place in the west and center areas of the southeastern coast of the KP. The variation of future SSH is projected to be 0.36 m (9.9%) in the bay. This future change may be due to the increase in the number of strong typhoons affecting the KP and the change of their typhoon tracks resulting from climate change. Storm surge risks around the KP in the future are expected to increase but the extent of that sensitively varies by location.

Fig. 8 shows the spatial distributions of SSH with 500-year return periods under past and future climate conditions as well as the future change of the SSH. The spatial patterns are similar to those of the 100-year return period, while the value of SSH increases around the coast under each climate condition. It is expected that the highest SSH will take place in a bay (marked with "B" in Fig. 8 (a)) with 4.92 m and 5.18 m under the past and future climate conditions, respectively. The variation is estimated to be 0.27 m (5.5%). As the return period of SSH extends from 100 to 500, the most vulnerable area tends to move to the east. As shown in Fig. 8 (c), the future change of SSH is projected to increase throughout the entire region except for some areas ranging between 127.9 °E to 128.2 °E and 34.8 °N to 35 °N, which is an area shifted by 0.4° to the east and 0.2° to the north, compared with the one of the 100-year return period. These differences of the highest SSHs and the vulnerable areas according to the return period of SSH result mainly from the changes in typhoon characteristics over time. Nonetheless, it is noted here that the projected future change of SSH with a 100-year return period is greater than that with a 500-year return period for a particular coastal site in the range between 127 °E to 127.6 °E and 34.5 °N to 34.8 °N. It is necessary to pay attention to such effects when selecting a return period of future SSH when coastal structures for disaster prevention against storm surges at the site are designed.

SSHs with particular return periods on specific locations in D4 are assessed. As shown in Fig. 9, all the locations have no significant changes for shorter return periods up to 50 years. However, the differences of SSHs between the past and future climate conditions become clearer for longer than the 100-years return periods except for a few location (e.g., Yoesu). For example, the future changes for Gadeokdo, Geomundo, Geojedo, and Goheung remain stable for a 30-year return period, then change. On the other hand, the noticeable future changes for Masan, Busan, and Tongyeong are shown after a 50-year return period. This future change is most apparent in Masan. There are no big differences projected until the 50-year return period. From then on there is striking variation between the past and future climates, with the maximum difference up to 0.88 m. In the historical record, the largest observed SSH was 2.34 m at Masan tidal station in 2003 (Yang et al., 2017). This value corresponded to one in the 600-year return period under past climate conditions, but it is expected to occur once every 200 years under future climate conditions. Minor future change is projected to be shown at Goheung, where the maximum difference caused by climate change is up to 0.3 m. On the other hand, the point with the smallest change under future climate conditions is Busan, where there is no noticeable difference throughout the entire

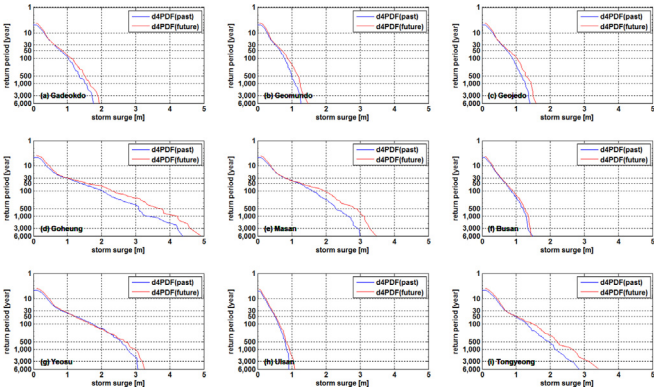

Fig. 9. Storm surge heights (m) with specific return periods at specific locations in the southeastern part of the Korean Peninsula. Each panel indicates the location; (a) Gadeokdo, (b) Geomundo, (c) Geojedo, (d) Goheung, (e) Masan, (f) Busan, (g) Yeosu, (h) Ulsan, and (i) Tongyeong whose locations are shown in Fig. 1 (right). Blue and red lines in the panel indicate storm surge heights with specific return periods under past and future climate conditions, respectively.

calculation period.

In the previous studies, results of a single experiment with short period have been used to project the future SSH with the long return period. Those, however, are involved with large uncertainties. The d4PDF makes it possible to project the future SSH with a long return period such as 100 years and 500 years, which is required for designing coastal structures like nuclear facilities. Fig. 10 shows comparisons of future SSH and its 95% confidence interval in terms of the number of ensemble experiments at *Yeosu* which is the location with the largest uncertainty range depending on the number of ensemble experiments (1) 10-experiment, (2) 50-ensemble experiment (i.e. sum of 25 arbitrary ensembles from d4PDF), and (3) 100-ensemble experiment (i.e. total d4PDF). For SSH with a 100-year return period, the results from the 100-ensemble experiment are shown in red in Fig. 10, with an estimate of 1.62 m and a 95% confidence interval range from 1.50 m to 1.73 m (ΔCI_{100} = 0.23 m). The results from the 50-ensemble and 10-ensemble experiments yield 1.69 m and 2.25 m for the 100-year return period, respectively. The 95% confidence intervals of those are in the ranges of 1.56 m–1.93 m (ΔCI_{50} = 0.38 m) and 1.38 m–2.82 m (ΔCI_{10} = 1.43 m), respectively. The difference of the uncertainty range between 100-ensemble and 10-ensemble experiments is 1.20 m. The results of the future SSHs and the its 95% confidence interval depending on the number of ensemble experiments at each location are shown in Table 3. From

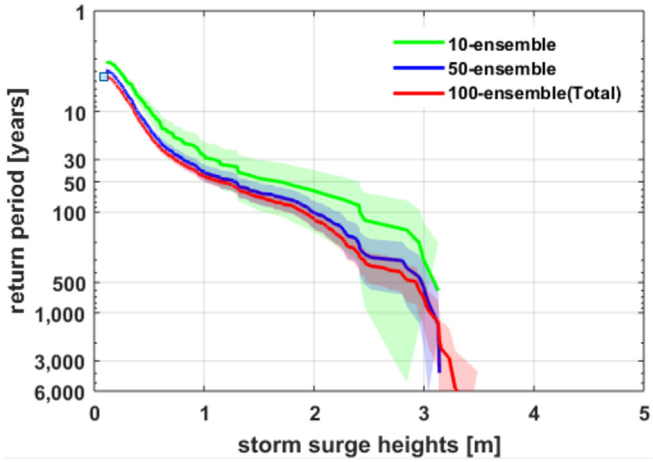

Fig. 10. Estimation of future storm surge heights with specific return periods at *Yeosu* using the results from total d4PDF (shown as a red line), 50 arbitrary ensembles from d4PDF (blue), and 10 ensembles from d4PDF (green). The shade indicates the 95% confidence intervals.

Table 3
Future storm surge heights with 100 years return period and its confidence interval at coastal locations.

Location	The number of ensemble experiments		
	10	50	100
Gadeokdo	1.26 m [1.01 m, 1.45 m]	1.15 m [1.00 m, 1.21 m]	1.06 m [1.00 m, 1.16 m]
Geomundo	0.97 m [0.80 m, 1.03 m]	0.90 m [0.84 m, 0.96 m]	0.86 m [0.84 m, 0.90 m]
Geojedo	1.14 m [0.91 m, 1.24 m]	1.02 m [0.93 m, 1.09 m]	0.99 m [0.94 m, 1.04 m]
Goheung	2.74 m [2.16 m, 3.25 m]	2.37 m [2.17 m, 2.75 m]	2.29 m [2.16 m, 2.40 m]
Masan	2.42 m [1.55 m, 2.96 m]	1.99 m [1.75 m, 2.23 m]	1.91 m [1.73 m, 2.01 m]
Busan	1.03 m [0.75 m, 1.14 m]	0.93 m [0.81 m, 0.99 m]	0.88 m [0.82 m, 0.93 m]
Yeosu	2.25 m [1.38 m, 2.82 m]	1.69 m [1.56 m, 1.93 m]	1.62 m [1.50 m, 1.73 m]
Ulsan	0.66 m [0.59 m, 0.70 m]	0.63 m [0.59 m, 0.67 m]	0.62 m [0.59 m, 0.64 m]
Tongyoung	1.76 m [1.28 m, 1.95 m]	1.52 m [1.27 m, 1.67 m]	1.44 m [1.26 m, 1.56 m]

these results it is obvious that large ensemble experiments can reduce the uncertainty in projection of future SSH.

As discussed above, it is expected that the aspect and variation of the future change of SSH for the southeastern area of the KP vary according to the place/region and its return period. This is thought to result from the increase of the number of strong typhoons affecting the KP and the change of typhoon tracks resulting from climate change. In addition, it is also expected that those in the western area of the KP differ depending on the place/region. The variation of the future change of SSH for the western area is projected to be greater than that of the southeastern area. However, since these findings for the western area are obtained from simulations with relatively coarse grids, it is necessary to further simulate using higher resolutions. A finer resolution may improve prediction accuracy by representing the coastal terrain and topography (Dietrich et al., 2011), despite the disadvantage of a higher computational cost.

4. Conclusions

This study projected the future storm surge heights (hereafter, SSHs) around the Korean Peninsula (hereafter, KP) and assessed the future change of these based on typhoon data from large ensemble experiments over 5000 years using a global atmospheric model of the Meteorological Research Institute with a 60 km horizontal resolution (hereafter, MRI-AGCM3.2H). Here, we used data of typhoons affecting the KP which pass through the region of 32 ˚N to 40 ˚N and 122 ˚E to 132 ˚E.

First, the reproducibility of the typhoon data in the present climate was estimated by comparing it with the observed typhoon data. The yearly average number of the typhoons was underestimated comparing to the observations, while the general trends of their tracks corresponded with the observations. The large ensemble experiments produced large samples of storm surge events under the past and future climate conditions. As the mean value of the minimum central pressure is smaller than that of the observations by 10.35 hPa, the values of minimum central pressure were linearly calibrated. The corrected typhoons were then used to project future storm surges.

Next, the future changes of typhoons were assessed. The number of typhoons approaching the KP was expected to be significantly reduced under future climate conditions by 38%. The general typhoon tracks including the locations of typhoon genesis and lysis were projected to shift to the northwest. The typhoons under the future climate are projected to be stronger than the ones under the past climate. Furthermore, the significant future change of the minimum central pressure is evident when intensifying typhoons whose pressures are smaller than 940 hPa.

Finally, the future change of SSH was projected by conducting a variety of storm surge simulations for the KP coast using the corrected typhoon data. The locations of the areas vulnerable to storm surge shift to the northern area of the western region and to the western area of the southern regions in the KP under future climate conditions. This characteristic of the future change to an area where higher SSHs occur coincide with that of the typhoon tracks. SSHs in the future climate are projected to increase in the KP except for in some areas in the south coast. The magnitude of the future change of SSH varies spatially. The maximum variation was estimated to be 0.36 m (9.9%) with a 100-year return period in the western area of the southeastern coast of the KP.

The present results in the study are able to be used for managing a coastal area and designing a design water level: (1) to identify areas vulnerable to storm surge on the regional or national scales, which is important for policy making to prioritize where to take action and to find appropriate site-specific solutions, (2) to estimate a design water level for coastal structure construction such as nuclear-related facilities which require a certain safety level for a long return period. In addition, the method used in this study may be applied to the projection of other variables (e.g. rainfall, wave). However, because this result is derived from only one GCM alone, further verification with a large ensemble using either another model or multi-models should be necessary for reducing uncertainties come from using single GCM.

Acknowledgement

This research was supported by the Integrated Research Program for Advancing Climate Models (TOUGOU) Program, Kakenhi (Grant-in-Aid of the Ministry of Education, Culture, Sports, Science, and Technology (MEXT), Japan) and the Supporting Technology Development Program for Disaster Management #2017-MPSS31-001 funded by the Ministry of the Interior and Safety (MOIS, Republic of Korea).

References

Camargo, S.J., 2013. Global and regional aspects of tropical cyclone activity in the CMIP5 models. J. Clim. 26, 9880–9902.
Deser, C., Phillips, A., Bourdette, V., Teng, H., 2012. Uncertainty in climate change projections: the role of internal variability. Clim. Dynam. 38, 527–546.
Dietrich, J.C., Zijlema, M., Westerink, J.J., Holthuijsen, L.H., Dawson, C., Luettich Jr., R.A., Jensen, R.E., Smith, J.M., Stelling, G.S., Stone, G.W., 2011. Modeling hurricane waves and storm surge using integrally-coupled, scalable computations. Coast. Eng. 58, 45–65.
Fujii, T., Mitsuda, Y., 1986. Synthesis of a stochastic typhoon model and simulation of typhoon winds. Annu. Disas. Prev. Res. Inst. Kyoto Univ. 29, 229–239.
Fujita, T., 1952. Pressure distribution within typhoon. Geophys. Mag. 23, 437–451.
General Bathymetric Chart of the Oceans (GEBCO). 2003. British Oceanographic Data Centre Centenary Edition.
Hamdi, Y., Bardet, L., Duluc, C.M., Rebour, V., 2014. Extreme storm surges: a comparative study of frequency analysis approaches. Nat. Hazards Earth Syst. Sci. 14, 2053–2067.
Harris, D.L., 1963. Characteristics of the Hurricane Storm Surge. Department of Commerce, Weather Bureau, Washington, D.C., pp. 139.
Kay, J.E., Deser, C., Phillips, A., Mai, A., Hannay, C., Strand, G., Arblaster, J.M., Bates, S.C., Danabasoglu, G., Edwards, J., Holland, M., Kushner, P., Lamarque, J.F., Lawrence, D., Lindsay, K., Middleton, A., Munoz, E., Neale, R., Oleson, K., Polvani, L., Vertenstein, M., 2015. The community earth system model (CESM) large ensemble project: a community resource for studying climate change in the presence of internal climate variability. Bull. Am. Meteorol. Soc. 96, 1333–1349.
Kim, S.Y., Yasuda, T., Mase, H., 2008. Numerical analysis of effects of tidal variations on storm surges and waves. Appl. Ocean Res. 30, 311–322.
Kim, S., Oh, J.H., Suh, K.D., Mase, H., 2017. Estimation of climate change impact on storm surges: application to Korean Peninsula. Coast. Eng. J. 59, 1740004.

Knapp, K.P., Kruk, M.C., Levinson, D.H., Diamond, H.J., Neumann, C.J., 2010. The international best track archive for climate stewardship (IBTrACS) unifying tropical cyclone data. Bull. Am. Meteorol. Soc. 91, 363–376.

Makkonen, L., 2006. Plotting position in extreme value analysis. J. Appl. Meteorol. Clim. 45, 334–340.

Mizuta, R., Murata, A., Ishii, M., Shiogama, H., Hibino, K., Mori, N., Arakawa, O., Imada, Y., Yoshida, K., Aoyagi, T., Kawase, H., Mori, M., Okada, Y., Shimura, T., Nagatomo, T., Ikeda, M., Endo, H., Nosaka, M., Arai, M., Takahashi, C., Tanaka, K., Takemi, T., Tachikawa, Y., Temur, K., Kamae, Y., Watanabe, M., Sasaki, H., Kitoh, A., Takayabu, I., Nakakita, E., Kimoto, M., 2016. Over 5000 years of ensemble future climate simulations by 60 km global and 20 km regional atmospheric models. Bull. Am. Meteorol. Soc. 98, 1383–1398.

Mori, N., Takemi, T., 2016. Impact assessment of coastal hazards due to future changes of tropical cyclones in the North Pacific Ocean. Weather Clim. Extremes 11, 53–69.

Murakami, H., Sugi, M., 2010. Effect of model resolution on tropical cyclone climate projections. SOLA 6, 73–76.

Murakami, H., Wang, T., Yoshimura, H., Mizuta, R., Sugi, M., Shindo, E., Adachi, Y., Yukimoto, S., Hosaka, M., Kusunoki, S., Ose, T., Kitoh, A., 2012a. Future changes in tropical cyclone activity projected by the new high-resolution MRI-AGCM. J. Clim. 25, 3237–3260.

Murakami, H., Mizuta, R., Shindo, E., 2012b. Future changes in tropical cyclone activity projected by multi-physics and multi-SST ensemble experiments using the 60-km-mesh MRI-AGCM. Clim. Dynam. 39, 2569–2584.

Murakami, H., Hsu, P.C., Arakawa, O., Li, T., 2014. Influence of model biases on projected future changes in tropical cyclone frequency of occurrence*. J. Clim. 27, 2159–2181.

Ogata, T., Mizuta, R., Adachi, Y., Murakami, H., Ose, T., 2016. Atmosphere-ocean coupling effect on intense tropical cyclone distribution and its future change with 60 km-AOGCM. Sci. Rep. 6, 29800.

Seo, S.N., 2008. Digital 30sec gridded bathymetric data of Korea marginal seas – KorBathy30s. J. Korean Soc. Coast. Ocean Eng. 20, 110–120.

Sterl, A., van den Brink, H., de Vries, H., Haarsma, R., van Meijgaard, E., 2009. An ensemble study of extreme storm surge related water levels in the North Sea in a change climate. Ocean Sci. 5, 369–378.

Strachan, J., Vidale, P.L., Hodges, K., Roberts, M., Demory, M.E., 2013. Investigating global tropical cyclone activity with a hierarchy of AGCMs: the role of model resolution. J. Clim. 26, 133–152.

Taylor, K.E., Stouffer, R.J., Meehl, G.A., 2012. An overview of CMIP5 and the experiment design. Bull. Am. Meteorol. Soc. 93, 485–498.

Vousdoukas, M.I., Voukouvalas, E., Annunziato, A., Giardino, A., Feyen, L., 2016. Projections of extreme storm levels along Europe. Clim. Dynam. 47, 3171–3190.

Wehner, M., Prabhat, Reed, K.A., Stone, D., Collins, W.D., Bacmeister, J., 2015. Resolution dependence of future tropical cyclone projections of CAM5.1 in the U.S. CLIVAR hurricane working group idealized configurations. J. Clim. 28, 3905–3925.

Weibull, W., 1939. A Statistical Theory of Strength of Materials. Generalstabens litografiska anstalts förlag, Stockholm.

Yang, J.A., Kim, S.Y., Mori, N., Mase, H. Projection of future changes of storm surges and assessment of its uncertainties based on ensemble experiments with multi-SST and greenhouse gas emission scenarios using single atmospheric global climate model. "Unpublished results-submitted".

Yang, J.A., Kim, S.Y., Mori, N., Mase, H., 2017. Bias correction of simulated storm surge height considering coastline complexity. Hydrol. Res. Lett. 11, 121–127.

Yasuda, T., Hayashi, Y., Mori, N., Mase, H., 2010. A stochastic typhoon model applicable to storm surge and wave simulations for climate change projection. J. Jpn. Soc. Civil Eng. B2 (Coast. Eng.) 66, 1241–1245.

Yasuda, T., Nakajo, S., Kim, S.Y., Mase, H., Mori, N., Horsburgh, K., 2014. Evaluation of future storm surge risk in East Asia based on state-of-the-art climate change projection. Coast. Eng. 83, 65–71.

Yoshida, K., Sugi, M., Mizuta, R., Murakami, H., Ishii, M., 2017. Future changes in tropical cyclone activity in high-resolution large-ensemble simulations. Geophys. Res. Lett. 44, 9910–9917.